A Transmission-Line-Type Model for Lightning Return Strokes with Branches

Amitabh Nag[1] and Vladimir A. Rakov[2]

1. Thunderstorm Systems and Data Division, Vaisala Inc., Louisville, Colorado, USA
2. Department of Electrical and Computer Engineering, University of Florida, Gainesville, Florida, USA

ABSTRACT: We examine the effect of channel branching on electric field waveforms produced by first return strokes in negative cloud-to-ground lightning using a modified transmission line model. From computed return stroke electric field waveforms it is found that the presence of an ungrounded branch results in sharper initial peak and a secondary peak in the falling part of the return stroke waveform. The time interval between the primary and secondary peaks depends upon the height of the branching point above ground and the speed at which the incident current wave moves upward from the ground. The presence of branch serves to slightly decrease the magnitude of the opposite polarity overshoot. The effects of the height of the branching point above ground, proportion of channel current flowing to the branch, and current reflections from the branch unconnected end are illustrated.

INTRODUCTION

Return-stroke models [e.g., Rakov and Uman, 1998] are used to relate the channel base current to the current distribution along the channel, which, in turn, can be used to calculate return-stroke electric and magnetic fields. Specifically, the transmission line (TL) model [Uman and McLain, 1969] has been demonstrated to work reasonably well in reproducing both close [e.g., Schoene et al., 2003] and relatively distant [e.g., Willett et al., 1988] fields for the first few microseconds of strokes in rocket-triggered lightning (which are thought to be similar to natural negative lightning subsequent strokes). Modifications to the TL model include a linear [MTLL, Rakov and Dulzon, 1987] and exponential [MTLE, Nucci et al., 1988] current decay with height. Both models are able to reproduce in return stroke electric and magnetic fields the sharp initial peak and zero-crossing within tens of microseconds of the initial peak at about 50 to 200 km.

In this study, we examine the effect of channel branching on distant electric field waveforms produced by first return strokes in negative cloud-to-ground lightning using a modified transmission line model. The effects of channel branches on return-stroke radiated fields have been theoretically studied by Le Vine and Meneghini [1978a], Vecchi et al. [1997], Lupo et al. [2000b], and Zich and Vecchi [2001]. One of the objectives of those studies was reproduction of pronounced fine structure observed in measured electric and magnetic fields of first return strokes. In this paper, we develop (or use) a simple model that allows us to examine the effects of a single branch, depending on its various parameters, with a view toward a better understanding of individual features of field waveforms, as opposed to their overall appearance.

∗ Contact information: Amitabh Nag, Vaisala Inc., Louisville, Colorado, USA, Email: amitabh.nag@vaisala.com

TRANSMISSION LINE MODEL

The transmission line (TL) model [Uman and McLain, 1969] for return strokes involves a current wave injected at the bottom of the lightning channel traveling upward at constant velocity v without attenuation or distortion. For the TL model the longitudinal current *i(z,t)* at any height z and any time t is related to the current at the channel origin (which in this case is at ground level) is given by Equation 1.

$$i(z,t) = i(0,\ t - \frac{z}{v}) \quad (1)$$

The current decay with height in the MTLL and MTLE models is represented by equations 2 and 3, respectively.

$$i(z,t) = (1 - \frac{z}{H}) i(0,\ t - \frac{z}{v}) \quad (2)$$

$$i(z,t) = e^{-\frac{z}{\lambda}} i(0,\ t - \frac{z}{v}) \quad (3)$$

H in Equation 2 is the assumed vertical channel length and λ in Equation 3 is the assumed decay height constant. The overall electric field waveforms at close distances are best reproduced by the MTLL model. However, for the initial few microseconds all three models predict essentially the same fields.

The general time-domain equation for computing the vertical electric field dE_z due to a vertical differential current element *idz* (channel segment of length *dz* carrying a uniform current *i(t)*) at a height *z* above a perfectly conducting ground plane for the case of an observation point P on the plane at a horizontal distance *r* from the dipole is given by [e.g., *Uman,* 1987]:

$$dE_z(r,t) = \frac{1}{2\pi\varepsilon_0}[\frac{(2z^2 - r^2)}{R^5(z)} dz \int_0^t i(z, \tau - \frac{R(z)}{c}) d\tau + \frac{(2z^2 - r^2)}{cR^4(z)} i(z, t - \frac{R(z)}{c}) dz - \frac{r^2}{c^2 R^3(z)} \frac{di(z, t - \frac{R(z)}{c})}{dt} dz] \quad (4)$$

where ε_0 is the electric permittivity of free space, R is the inclined distance from the dipole to the observation point, which is given by $R = \sqrt{z^2 + r^2}$.

From Equation 4, the total electric field at the observation point for a finite-length vertical channel whose lower and upper ends are at altitudes of z = 0 and z = *H*, respectively, is given by:

$$E_z(r,t) = \frac{1}{2\pi\varepsilon_0} \int_0^H [dz \frac{(2z^2 - r^2)}{R^5(z)} \int_0^t i(z, \tau - \frac{R(z)}{c}) d\tau + \frac{(2z^2 - r^2)}{cR^4(z)} i(z, t - \frac{R(z)}{c}) dz - \frac{r^2}{c^2 R^3(z)} \frac{di(z, t - \frac{R(z)}{c})}{dt} dz] \quad (5)$$

We used the Heidler function [Heidler, 1985] to represent the channel-base current waveform. It is given by:

$$i(0,t) = \frac{I_0}{\eta} \frac{(\frac{t}{\tau_1})^n}{(\frac{t}{\tau_1})^n + 1} e^{-\frac{t}{\tau_2}} \quad (6)$$

where I_0 = 20 kA, η = 0.5, n = 10, τ_1 = 4 μs, and τ_2 = 100 μs. The current waveform is shown in Figure 1 and has a peak of about 37 kA and a zero-to-peak risetime of 6.6 μs.

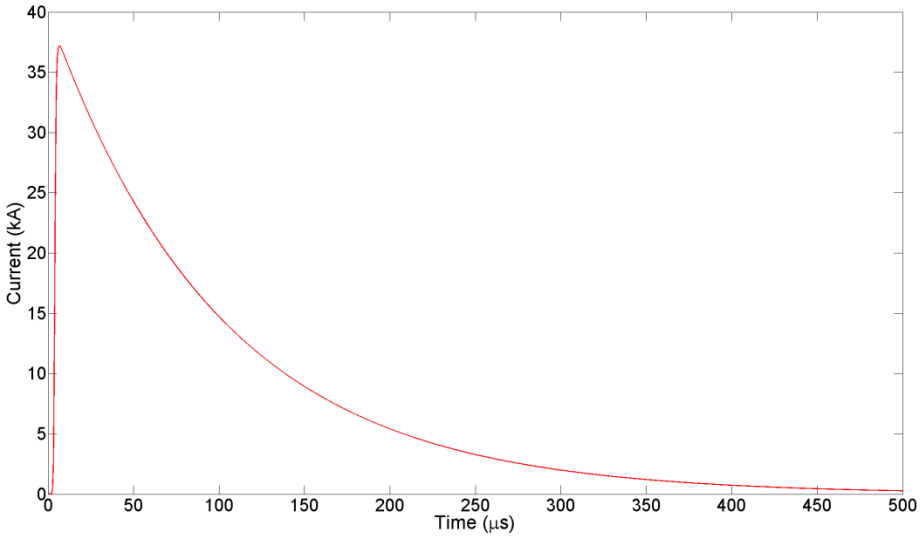

Figure 1. The incident return stroke current waveform computed using the Heidler function that is used in this study shown on a 500 μs timescale. The current peak is about 37 kA and the zero-to-peak risetime is 6.6 μs. The half-peak width is 72 μs. This current waveform is representative of negative first return strokes.

BRANCHING OF RETURN STROKE CHANNEL

Figure 2a shows the geometry of the lightning return stroke channel considered in this paper. The return stroke channel consists of a main channel that extends between the ground and the cloud charge source, and, additionally, includes an ungrounded branch. Figure 2b shows the simplified version of this channel geometry. The main channel and the branch are considered to be vertical and connected by a short horizontal channel segment. The branching point is at height h_b above ground and has a length of l_b such that $h_b > l_b$. The incident return stroke current *i* travels upward from ground along the main channel. Upon reaching the branching point B, the incident current splits into two parts, i_1 and i_2, such that $i_B = i_1 + i_2$, where i_B is the incident current peak at B. While i_1 continues upward along the main channel, i_2 travels downward along the ungrounded branch. This is equivalent to the scenario shown in Figure 2c, in which incident current *i* travels upward along the entire length of the main channel, and, the instant the incident current *i* reaches B, two elevated current sources placed at B launch currents $-i_2$ and i_2 upward along the main channel and downward along the ungrounded branch, respectively. We use equations 2 and 5 to

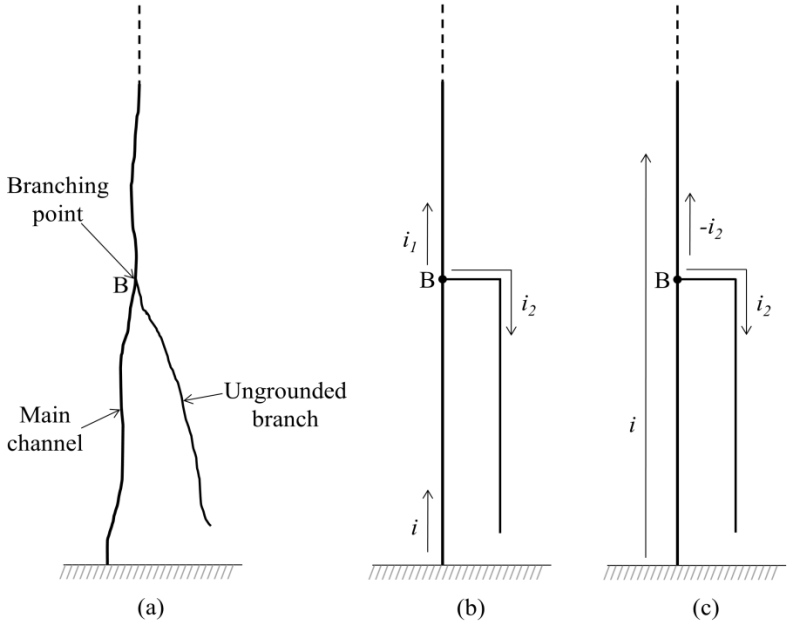

Figure 2. (a) The geometry of the lightning channel considered in this paper. The channel consists of a main channel that extends between the ground and the cloud charge source, and additionally, includes an ungrounded branch. (b) The simplified version of the channel geometry shown in (a). Both the main channel and the branch are considered to be vertical and separated by a short horizontal channel segment. (c) Configuration equivalent to (b) that was used in computing fields. See text for details.

compute the vertical component of electric field at an observation point at distance r from the lightning channel for each of the three currents flowing through various channel segments described above. The sum of the three electric fields gives us the total vertical electric field at ground due to current flowing through the main channel and branch for the geometry shown in Figure 2c. Contribution to the vertical electric field from the horizontal channel segment is neglected. Further, the length of the horizontal section is assumed to be much smaller than r, so that all the field components are computed at that distance.

MODELING RESULTS

Figure 3a shows the MTLL-model-computed return stroke electric field at a distance of 200 km for a straight vertical channel with no branching (blue dashed line) and for the channel geometry shown in Figure 2c (black solid line). The length of the main channel is assumed to be 8 km, the current velocity v = 1.5 x 10^8 m/s for all channel segments, the branching point B is at height h_b = 500 m above the ground surface, and the length of the ungrounded branch l_b = 450 m. The length of the horizontal section of the channel between the branching point B on the main channel and the top of the vertical ungrounded branch is assumed to 100 m. The current is assumed to decay linearly to zero (MTLL, equation 2) at the upper

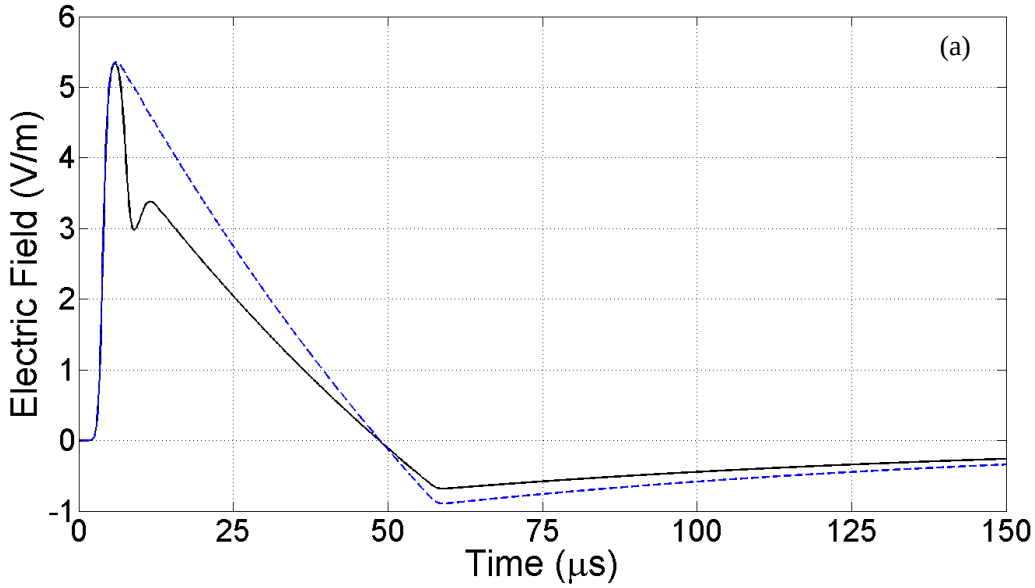

Figure 3. (a) The MTLL-model-computed return stroke electric field at a distance of 200 km for a straight vertical channel with no branching (blue dashed line) and for the channel geometry shown in Figure 2c (black solid line) shown on a 150 μs timescale. The presence of branch served to slightly decrease the magnitude of the opposite polarity overshoot.

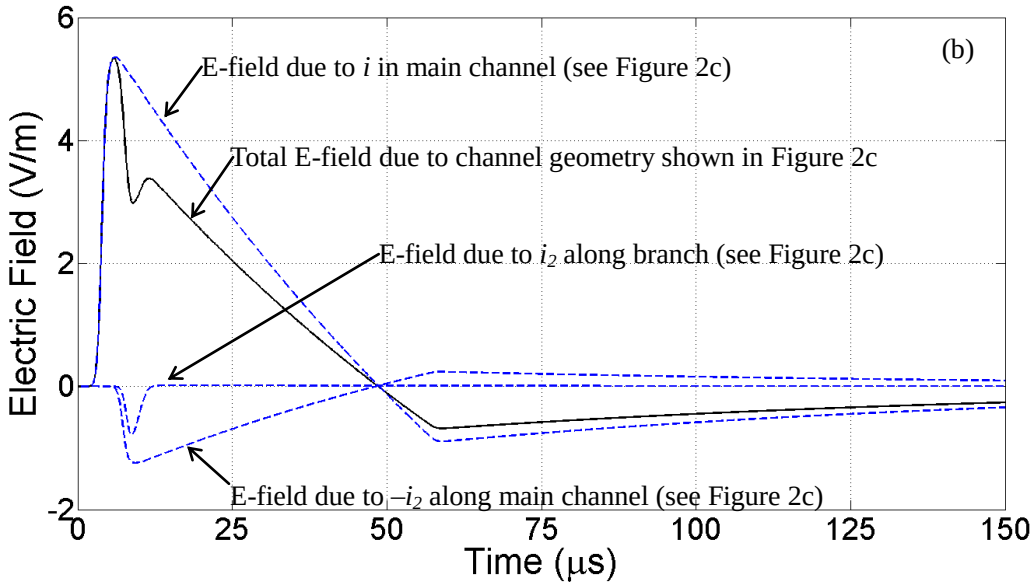

Figure 3. (b) The solid line shows the same waveform as in Figure 3a but additionally showing the contributions to the total electric field (waveforms shown with dashed lines) from the individual current components shown in Figure 2c.

end of the main channel and the lower end of the ungrounded branch. The ratio of i_2 to i_1 is assumed to be 0.25.

As can be seen from Figure 3a, the presence of an ungrounded branch produces sharper initial peak and a secondary peak in the falling part of the return stroke waveform. Additionally, Figure 3b shows the

contributions to the total electric field from the individual current components (waveforms shown with dashed lines) shown in Figure 2c. The time interval between the primary and secondary peaks depends upon the height of the branching point above ground and the speed at which the incident current moves upward from the ground. The presence of branch served to slightly decrease the magnitude of the opposite polarity overshoot. Note that the only effect of the length of the horizontal section on the overall electric field is to increase the time interval between the primary and secondary field peaks (by 100 m /1.5 x 10^8 m/s = 0.67 μs in the example shown in Figure 3a).

DISCUSSION

The waveform shown with solid line in Figure 4 represents the MTLL-model-computed return stroke electric field at a distance of 200 km for the channel geometry shown in Figure 2c and the same parameters as those used to compute the solid line curve in Figure 3a, but with i_2/i_1 = 0.5. The electric field waveform for i_1/i_2 = 0.25 (same as in Figure 3a) is also shown with dashed line for comparison. From Figure 4 it appears that as the i_2/i_1 ratio increases (increasing the portion of the total current i flowing to the branch), the field decrease between the initial and secondary peaks becomes larger and the magnitude of secondary peak becomes smaller (relative to zero level).

Figure 5 shows the computed return stroke electric field at a distance of 200 km for the same parameters as in Figure 4, but with h_b = 1400 m above the ground surface and the length of the ungrounded branch l_b = 1350 m (solid line). Also shown with dashed line is the electric field waveform for h_b = 500 m for comparison. As expected, the secondary peak appears later in the waveform when the height of the branching point is higher. Additionally, the electric field decreases to zero prior to the secondary peak (at 15 μs). Field decrease to zero (or even a brief polarity change) prior to "normal" zero-crossing is sometimes observed in measured electric field waveforms and may be due to the presence of a long branch.

In all the above computations of return stroke electric fields we have assumed that the current in the downward branch decays linearly to zero at the bottom of the branch. Next, we assume that the current injected into the branch decays linearly to zero after it has traveled downward along the branch, been reflected off bottom (open-circuited) end of the branch, and then travelled back to the branching point on the main channel. Figure 6 shows the computed return stroke electric fields with (black solid line) and without (blue dashed line) reflection at the bottom end of the branch. All parameters are the same as those used to compute the black-solid-line curve in Figure 3a. Reflection at the branch-end has very small effect on the overall return stroke waveform but causes an increase in the amplitude of the secondary peak.

We now additionally consider the effect of a long horizontal section of the channel attached at the

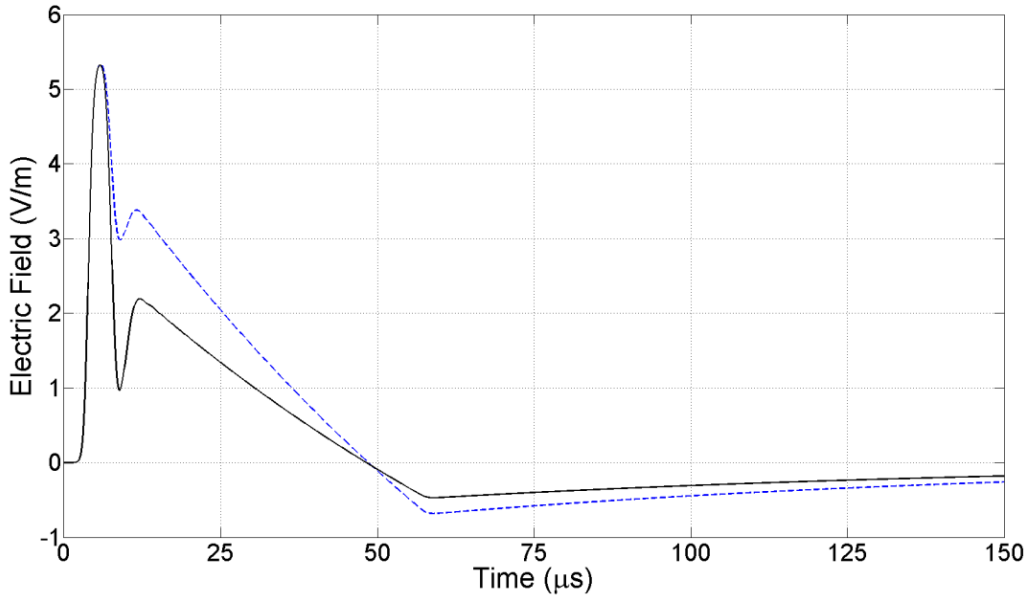

Figure 4. The MTLL-model-computed return stroke electric field at a distance of 200 km for the channel geometry shown in Figure 2c and the same parameters as those used to compute the solid line curve in Figure 3a, but with i_2/i_1 = 0.5 (solid line). The electric field waveform for i_1/i_2 = 0.25 (same as in Figure 3a) is also shown (dashed line) for comparison. The time-window shown is 150 μs.

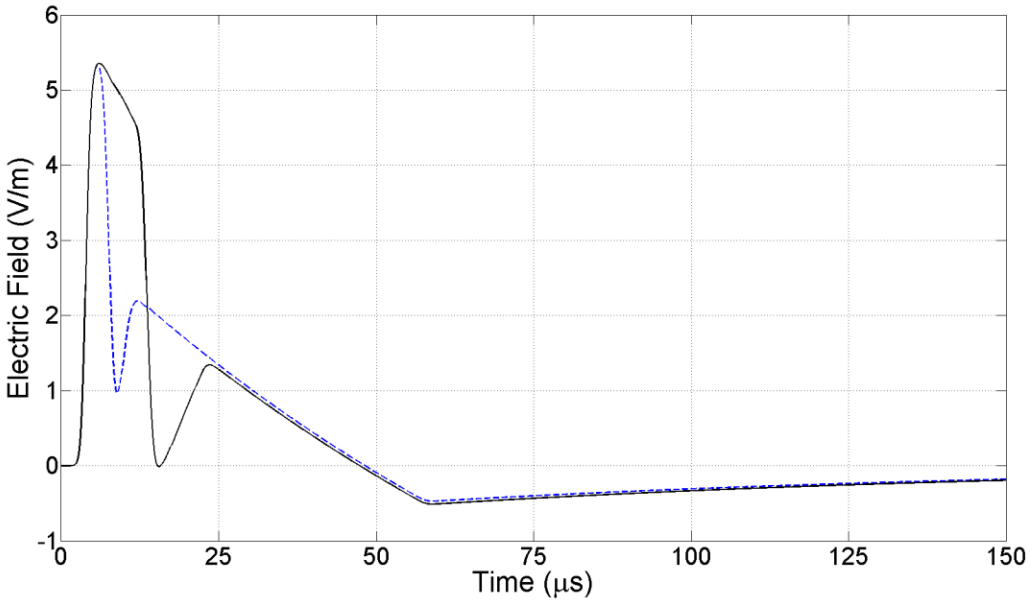

Figure 5. The MTLL-model-computed return stroke electric field at a distance of 200 km for the same parameters as in Figure 4, but with h_b = 1400 m above the ground surface and the length of the ungrounded branch l_b = 1350 m (solid line). Also shown is the electric field waveform for h_b = 500 m (dashed line) for comparison. The time-window shown is 150 μs.

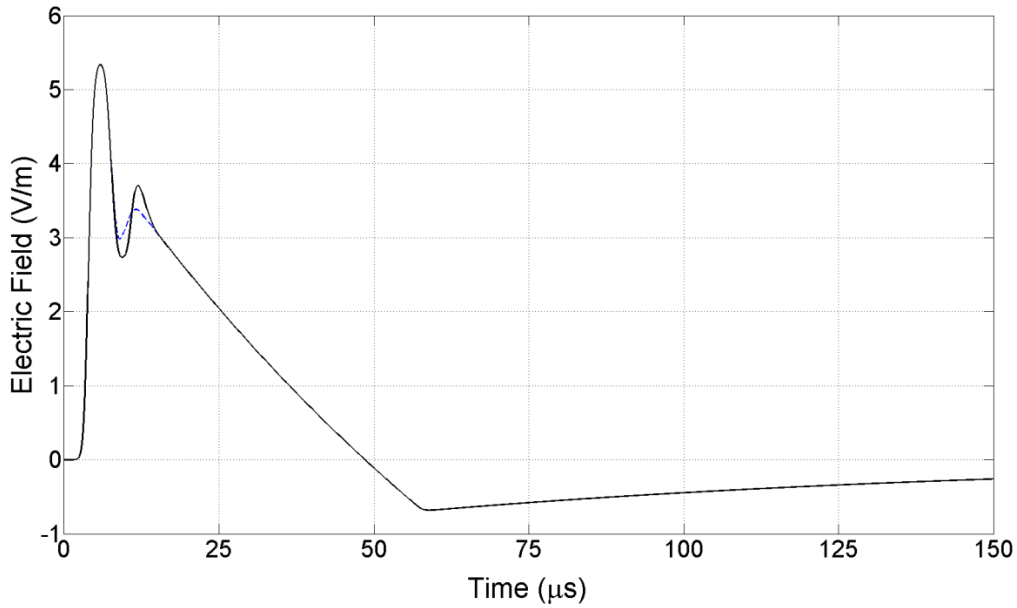

Figure 6. The MTLL-model-computed return stroke electric fields with (black solid line) and without (blue dashed line) reflection at the bottom end of the branch. All parameters are the same as those used to compute the solid black line curve in Figure 3a. Reflection at the branch-end causes an increase in the amplitude of the secondary peak in the return stroke waveform. The time-window shown is 150 μs.

upper end of a vertical return stroke channel on the return stroke electric field waveform. The channel geometry is shown in Figure 7a. (Note that Cooray et al. [2008] suggested that a horizontal channel section in the cloud is the reason for an opposite polarity overshoot in distant electric field waveforms produced by lightning return strokes.) The incident return stroke current *i* travels upward from ground along the channel. Upon reaching point C, the incident current flows along the horizontal branch. Figure 7b shows the return stroke electric field waveform at 200 km in the presence of the horizontal section (solid line). The lengths of the vertical and horizontal channel sections are assumed to be 8 km each, the current velocity $v = 1.5 \times 10^8$ m/s, and the current is assumed to decay linearly to zero at the far-end of the horizontal branch. Contribution to the vertical electric field from the horizontal channel segment is neglected. The return stroke field waveform shows an opposite polarity overshoot following the zero crossing, which is slightly more pronounced than seen in the blue dashed line curve in Figure 3a (the ratio of the opposite polarity overshoot to initial peak in the former is 0.26 versus 0.17 in the latter). Also shown for comparison is the return stroke waveform (dashed line) in the presence of a branch (shown in Figures 2b and c) attached to the main channel at a height of 500 m above ground, in addition to the long horizontal channel section shown in Figure 7a.

SUMMARY

We extend TL-type models to include a long branch and examine its effect on distant electric field waveforms produced by first return strokes in negative cloud-to-ground lightning.

The presence of an ungrounded branch produces sharper initial peak and a secondary peak in the

falling part of the return stroke waveform. The time interval between the primary and secondary peaks depends upon the height of the branching point above ground and the speed at which the incident current wave moves upward from the ground. The presence of branch served to slightly decrease the magnitude of the opposite polarity overshoot. The effects of the height of the branching point above ground, proportion of channel current flowing to the branch, and current reflections from the branch bottom are examined. The effect of the presence of a long horizontal section connected at the upper end of a vertical return stroke channel is additionally considered.

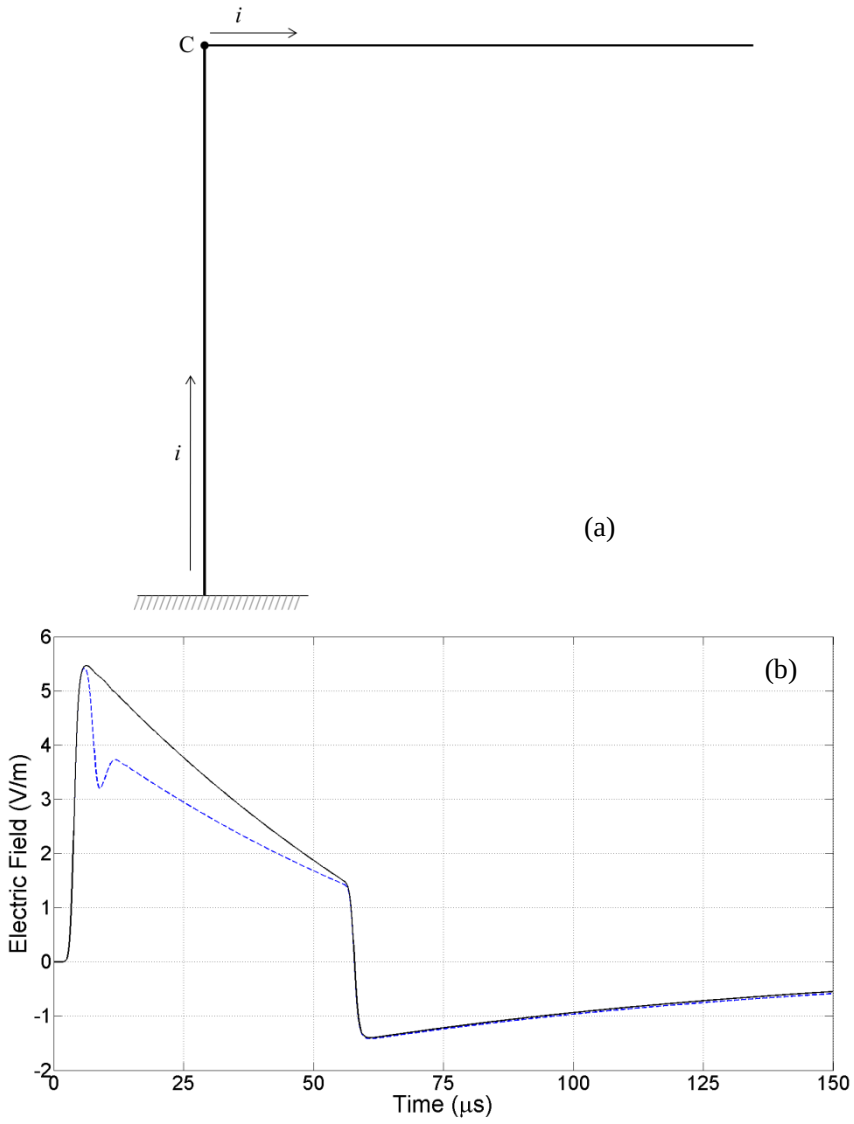

Figure 7. (a) The channel geometry including a long horizontal section attached at the upper end of a vertical return stroke channel. (b) The MTLL-model-computed return stroke electric field at a distance of 200 km for the geometry shown in (a) (solid line), and for the geometry including both the horizontal channel section and a branch connected at 500 m (see Figure 2) (dashed line). The time-window shown is 150 μs.

REFERENCES

Cooray, V., V. A. Rakov, F. Rachidi, R. Montano, and C. A. Nucci (2008), On the relationship between the signature of close electric field and the equivalent corona current in lightning return stroke models, *IEEE Trans on EMC, 50*, No. 4, 921-927.

Heidler, F. (1985), Travelling current source model for LEMP calculation, Proc. of *6th Intl. Symp. on Electromagnetic Compatibility*, Zurich, Switzerland, pp. 157–162.

Le Vine, D. M., and R. Meneghini (1978a), Electromagnetic fields radiated from a lightning return stroke: application of an exact solution to Maxwell's equations, *J. Geophys Res., 83*, 2377-84.

Lupo, G., C. Petrarca, V. Tucci, and M. Vitelli (2000b), EM fields associated with lightning channels: on the effect of tortuosity and branching, *IEEE Trans. Electromagn. Compat., 42*, 394-404.

Nucci, C. A., C. Mazzetti, F. Rachidi, and M. Ianoz (1988), On lightning return stroke models for LEMP calculations, in Proc. *19th Int. Conf. Lightning Protection*, Graz, Austria.

Rakov, V. A., and A. A. Dulzon (1984), On latitudinal features of thunderstorm activity, *Meteor. Gidrol., 1*, 52–57.

Rakov, V. A., and M.A. Uman (1998), Review and evaluation of lightning return stroke models including some aspects of their application, *IEEE Trans. on EMC, 40*, No. 4, part II, Special Issue on Lightning, pp. 403–426.

Schoene, J., M. A. Uman, V. A. Rakov, K. J. Rambo, J. Jerauld, and G. H. Schnetzer (2003), Test of the transmission line model and the traveling current source model with triggered lightning return strokes at very close range, *J. Geophys. Res., 108* (D23), 4737, doi:10.1029/2003JD003683.

Uman, M. A. (1987), The Lightning Discharge, Dover Publications, Inc., Mineola, New York.

Uman M. A., and D. K. McLain (1969), Magnetic field of the lightning return stroke, *J. Geophys. Res., 74*, 6899–6910.

Vecchi, G., D. Labate, and F. C. Canavero (1997), A study of the effect of channel branching on lightning radiation, in Proc. of *12th Intl. Symp. on Electromagn. Compat*., Zurich, Switzerland, pp. 65-70.

Willett, J. C., V. P. Idone, R. E. Orville, C. Leteinturier, A. Eybert-Berard, L. Barret, and E. P. Krider (1988), An experimental test of the "transmission-line model" of electromagnetic radiation from triggered lightning return strokes, *J. Geophys. Res., 93* (D4), 3867–3878.

Zich, R. E., and G. Vecchi (2001), Lightning discharge on a branched channel, in Proc. of *14th Intl. Symp. on Electromagn. Compat.*, Zurich, Switzerland, pp. 299-304.